SMiRT-12 / K. Kussmaul (Editor)

F01/1

COMPUTATION OF PRINCIPAL STRESSES AND STRESS INTENSITY OF A NOZZLE ON A SPHERICAL PRESSURE VESSEL

B.C. Sun[1], B.L. Lyow[2] and B. Koplik[3]

[1]Dept. of Engineering Technology, New Jersey Institute of Technology, Newark, New Jersey, USA, [2]Becht Engineering, Liberty Corner, New Jersey, USA, [3]Department of Mechanical and Industrial Engineering, New Jersey Institute of Technology, Newark, New Jersey, USA

ABSTRACT

This paper presents a Stress Computation Table that systematically computes the local stresses at various locations of the sphere-nozzle intersection. The six components of external loading are: radial load, two overturning moments, two horizontal shear forces, and a torsional moment. The radial and overturning moments induce local membrane and bending stresses in both the circumferential and meridional directions of the sphere around the nozzle. The shear forces and torsional moment produce local shear stresses. In addition, the shear forces induce local membrane and bending stresses around the nozzle. The local stress factors from each external loading component are taken from recent publications by Lyow, Sun and Koplik who have studied this subject through the use of the finite element method. These factors are a function of the nozzle-sphere geometrical parameters, beta, ß,(nozzle radius / sphere radius) and gamma, γ, (sphere radius / thickness), with the beta value ranging from 0.1 to 0.5, and the gamma value ranging from 10 to 100. The Stress Table summarizes all the normal and shear stresses at eight different locations around the nozzle, and finally the principal stresses and stress intensity are computed. The stress factor plots from previous publications are replotted in this paper to provide a handy reference as well as consistency. A numerical sample employing a FORTRAN program is also given.

INTRODUCTION

It is well established that Welding Research Council Bulletin 107 published in 1968 [1] has been the most popular stress calculation guide for pressure vessel designers to analyze local stresses on vessel-nozzle connections due to external loadings. It is also known that the theoretical base of Welding Research Council Bulletin 107 for the sphere-nozzle connection was from the Bessel function solutions derived by Bijlaard [2],[3]. He used a uniformly distributed load applied on a circular region of the sphere to simulate the radial loading on the nozzle, and then used a linearly distributed load on the same region to simulate the bending moment loading on the nozzle. Although it did not actually simulate the real nozzle opening on the vessels, still, the loading distributions on the vessel-nozzle juncture gave a good analytical solution for a solid cylindrical support attached to the vessels. Finally, the analytical solutions were not available to determine the induced local stresses due to the external shear forces and the torsional moment. The shear stress calculations are only approximations.

In recent years investigators have used finite elements to model the real vessel-nozzle connections and the external loadings to study these local stresses. In 1990, Lyow, Sun and Koplik [4] presented their results on local stresses around a sphere-nozzle connection when it is subjected to an external radial load. Their local stress results are presented in the form of stress factors which are defined based on the stress calculations for pipe-nozzle from the Welding Research Council Bulletin 107. These stress factors are then plotted in terms of beta, β, (nozzle radius/sphere radius) and gamma, γ, (sphere radius / thickness). They later extended their studies to include the bending moment, torsional moment and shear force [5]. In the latter work they discovered that the external shear force induces not only shear stress, but also bending and membrane stresses at the juncture, and all these stresses are not uniformly distributed around the nozzle. These results have substantially improved the local stress calculations previously available.

To facilitate the local stress computations from the above mentioned work, authors of the present paper developed a Stress Computation Table that tabulates all the local stress components induced by the external loadings, and preassigned an appropriate stress sign to each stress entry. One notes that the sign of each local stress component depends on the sense of the applied load and stress location on the nozzle. After the entry of the local stress components, the Table summarizes them in the circumferential, meridional and radial directions of the sphere, respectively, and it finally computes the stress intensity at eight different locations around the nozzle.

COMPUTATIONAL TABLE FOR SPHERE-NOZZLE

Figure 1 shows a typical sphere-nozzle connection with six components of external loading. Each loading component that contributes to the local stresses are listed as follows:

1) Radial load, P, bending moments, M_Z and M_X induce both membrane and bending stresses in both the circumferential and meridional directions around the juncture.

2) Horizontal shear forces, V_Z and V_X, induce shear stress on the nozzle symmetric plane which is perpendicular to the direction of the applied force. These shear forces also induce the normal stresses mentioned above, however, these stresses are significant only on the nozzle symmetric plane that lies in the same direction as the applied force.

3) Torsional moment, M_T, induces uniform shear stress around the juncture.

The local stress computation table for the sphere-nozzle is

presented in Table I. One notes that the stress components follow the local coordinates only. All the stress factors, calculated and plotted by Lyow, Sun, and Koplik [4] & [5], are repeated in this paper as shown in the figures as follows:
Figures SP-1 to SP-4: radial load, P.
Figures SM-1 to SM-4: overturning moment, M_X or M_Z.
Figures SV-1 to SV-5: shear force, V_X or V_Z.
Figures ST-1 : torsional moment, M_T.

NUMERICAL EXAMPLE

A spherical pressure vessel with an outside diameter of 101 inches and a one inch thickness, has an 11 inch outside diameter nozzle. It is subjected to an internal pressure of 50 psi and the following loading components:

P =	4000 lb (downward),	M_Z =	5000 in-lb,
M_X =	5000 in-lb,	M_T =	5000 in-lb,
V_Z =	3000 lb,	V_X =	-4000 lb (+ x direction)

In this example, the pipe radius, R_m = 50. in, the thickness of the vessel and the nozzle, T = t = 1.0 in. and the nozzle radius, r_m = 5.0 in. As a result, beta, ß, (r_m/R_m) = 0.1 and gamma, γ , (R_m/T) = 50. From the stress factor figures, one obtains various stress factors through interpolation. The pressure membrane stress is 1250 psi in the shell of the vessel, the components of all local stress are calculated according to formulas listed in Table I. The resulting stresses at eight different locations around the juncture are tabulated in Table II where the principal stresses and the maximum stress intensity are also determined.

DISCUSSION

When using the above results one notes that the finite element models from [4] and [5] have assumed the nozzle-sphere intersection has no fillet weld. Therefore, the actual vessel local stresses around the nozzle with a fillet weld or pad would be lower.

The thickness of the nozzle and the sphere are assumed to be the same. Since the nozzle has a much smaller diameter than the vessel, therefore the nozzle has much more material reserve than the vessel itself and the local stress computed in this paper is for the sphere only.

The stress concentration factors, K_b(for bending stresses), and K_n(for normal stresses), are taken as unity in the numerical example. The reader may refer to Reference [1] to determine the appropriate stress concentration factors.

One further notes that the pressure stresses are the primary stresses. One may simply make zero value entry to exclude these pressure stress components.

Due to the page limitation, the FORTRAN computer program for the above computation is not included. The reader may contact the authors for an execution program diskette which runs on IBM compatible personal computers.

REFERENCES

[1] Wichman, K.R., Hopper, A. G., Mershon, J. L., 1968, "Local Stresses in Spherical and Cylindrical Shells due to External Loadings", Welding Research Council Bulletin 107, last revision in March 1979.

[2] Bijlaard, P. P., 1959, "Stresses in a Spherical Vessel for Radial Loads Acting on a Pipe", Welding Research Council Bulletin No. 49, pp 1-30, issued in April.

[3] Bijlaard, P. P., 1959, "Stresses in a Spherical Vessel for External Moments Acting on a Pipe", Welding Research Council Bulletin No. 49, pp 31-62, issued in April.

[4] Lyow, B. L., Sun, B. C., and Koplik, B., 1990, "Finite Element Method to Determine the Localized Stresses and Spring Constants of a Spherical Shell with a Nozzle Attachment under Radial Loading", "Analysis of Pressureí Vessel and Heat Exchanger Components", ASME PVP Vol. 194, pp. 1-7.

[5] Lyow, B. L., Sun, B. C., and Koplik, B., 1991, "Local Stresses and Spring Constants of Sphere-Nozzle Connection due to an Overturning Moment, a Torsional Moment and a Horizontal Shear Force by Finite Element Approach", "Pressure Vessel and Components", ASME PVP Vol. 217, pp. 21-31.

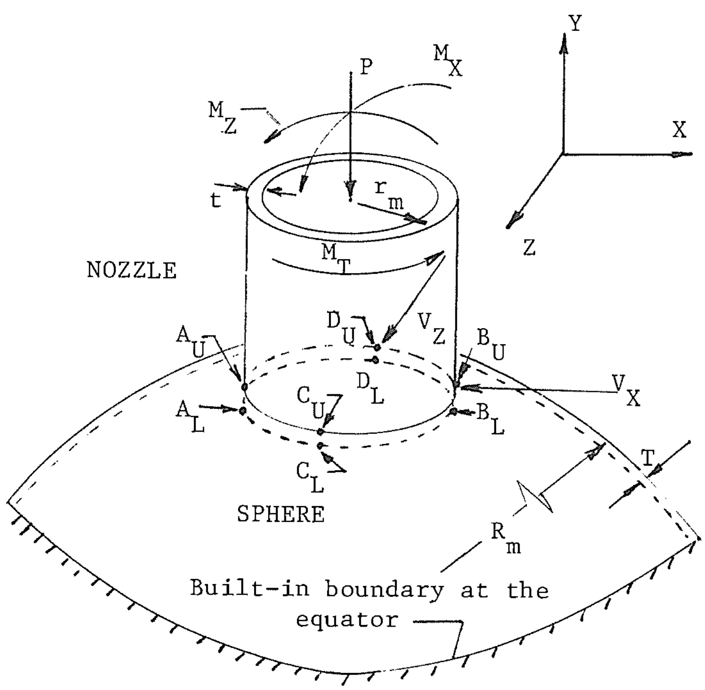

Figure 1. Sphere with a nozzle attachment subjected to six components of external loading.

PROBLEM NO. = 1	DATE: 1/31/1993		
SPHERE OD, IN = 101.00	SPHERE THICKNESS, IN.	=	1.00
NOZZLE OD, IN = 11.00	INTERNAL PRESSURE, PSI	=	50.00
RADIAL FORCE, LB. = 5000.00	MX MOMENT, IN-LB.	=	4000.00
Z MOMENT, IN-LB = 5000.00	X-AXIS SHEAR FORCE, LB.	=	-4000.00
Z-AXIS SHEAR FORCE, LB. = 3000.00	TORSIONAL MOMENT, IN-LB.	=	5000.00

BETA = .100, GAMMA = 50.000

STRESS CONCENTRATION FACTORS: Kn = 1.000, Kb = 1.000

SP-3 = .10311,	SP-1 = .09968,	SM-3 = .01430,	SM-1 = .03480
SV-3 = .01400,	SV-1 = .01584,	SP-4 = .04728,	SP-2 = .28028
SM-4 = .01100	SM-2 = .08800,	SV-4 = .02468,	SV-2 = .02990
ST-1 = .00443,	SV-5 = .02750		

SUMMARY OF LOCAL STRESSES, PRINCIPAL STRESSES AND STRESS INTENSITY

FIG.	STRESS	AU	AL	BU	BL	CU	CL	DU	DL
SP-3	P (NORMAL)	-516.	-516.	-516.	-516.	-516.	-516.	-516.	-516.
SP-1	P (BENDING)	-498.	498.	-498.	498.	-498.	498.	-498.	498.
SM-3	MX (NORMAL)					-57.	-57.	57.	57.
SM-1	MX (BENDING)					-139.	139.	139.	-139.
SM-3	MZ (NORMAL)	-72.	-72.	72.	72.				
SM-1	MZ (BENDING)	-174.	174.	174.	-174.				
SV-3	VX (NORMAL)	-56.	-56.	56.	56.				
SV-1	VX (BENDING)	63.	-63.	-63.	63.				
SV-3	VZ (NORMAL)					42.	42.	-42.	-42.
SV-1	VZ (BENDING)					48.	-48.	-48.	48.
P Rm /	(2 T)	1250.	1250.	1250.	1250.				
SUM.	CIRCUM.	-2.	1216.	474.	1250.	129.	1309.	343.	1156.
SP-4	P (NORMAL)	-236.	-236.	-236.	-236.	-236.	-236.	-236.	-236.
SP-2	P (BENDING)	-1401.	1401.	-1401.	1401.	-1401.	1401.	-1401.	1401.
SM-4	MX (NORMAL)					-44.	-44.	44.	44.
SM-2	MX (BENDING)					-352.	352.	352.	-352.
SM-4	MZ (NORMAL)	-55.	-55.	55.	55.				
SM-2	MZ (BENDING)	-440.	440.	440.	-440.				
SV-4	VX (NORMAL)	99.	99.	-99.	-99.				
SV-2	VX (BENDING)	120.	-120.	-120.	120.				
SV-4	VZ (NORMAL)	-74.	-74.	74.	74.				
SV-2	VZ (BENDING)	90.	-90.	-90.	90.				
P Rm /	(2 T)	1250.	1250.	1250.	1250.				
SUM.	MERIDO.	-664.	2779.	-111.	2051.	-768.	2559.	-7.	2271.
ST-1	MT (SHEAR)	22.	22.	22.	22.	22.	22.	22.	22.
SV-5	VZ (SHEAR)	83.	83.	-83.	-83.				
SV-5	VX (SHEAR)					110.	110.	-110.	-110.
SUM.	SHEAR	105.	105.	-60.	-60.	132.	132.	-88.	-88.
SIGMA1		14.	2786.	480.	2055.	148.	2572.	363.	2278.
SIGMA2		-680.	1210.	-116.	1245.	-786.	1296.	-27.	1150.
SIGMA3			-50.		-50.		-50.		-50.
ST. INTENSITY		694.	2836.	596.	2105.	934.	2622.	390.	2328

MAXIMUM STRESS INTENSITY = 2836. PSI.

Table II. Numerical Stress Computations for Sphere-Nozzle

FIGURE	stress factor	component of local stresses	A_U	A_L	B_U	B_L	C_U	C_L	D_U	D_L
SP-3	$K_{c,m}T^2$	$K_n(K_{c,m}T^2)P/T^2$	-	-	-	-	-	-	-	-
SP-1	$K_{c,b}T^2$	$K_b(k_{c,b}T^2)P/T^2$	-	+	-	+	-	+	-	+
SM-3	$K_{c,m}T^2$	$K_n(K_{c,m}T^3)M_x/T^3$	\\\	\\\	\\\	\\\	-	-	+	+
SM-1	$K_{c,b}T^3$	$K_b(K_{c,b}T^3)M_x/T^3$	\\\	\\\	\\\	\\\	-	+	+	-
SM-3	$K_{c,m}T^3$	$K_n(K_{c,m}T^3)M_z/T^3$	-	-	+	+	\\\	\\\	\\\	\\\
SM-1	$K_{c,b}T^3$	$K_b(K_{c,b}T^3)M_z/T^3$	-	+	+	-	\\\	\\\	\\\	\\\
SV-3	$K_{c,m}T^2$	$K_n(K_{c,m}T^2)V_x/T^3$	+	+	-	-	\\\	\\\	\\\	\\\
SV-1	$K_{c,b}T^2$	$K_b(K_{c,b}T^2)V_x/T^3$	-	+	+	-	\\\	\\\	\\\	\\\
SV-3	$K_{c,m}T^2$	$K_n(K_{c,m}T^2)V_z/T^2$	\\\	\\\	\\\	\\\	+	+	-	-
SV-1	$K_{c,b}T^2$	$K_b(K_{c,b}T^2)V_z/T^2$	\\\	\\\	\\\	\\\	+	-	-	+
P		$pR_m/(2T)$								
Sum of circum. stresses										
SP-4	$K_{m,m}T^2$	$K_n(K_{m,m}T^2)P/T^2$	-	-	-	-	-	-	-	-
SP-2	$K_{m,b}T^2$	$K_b(K_{m,b}T^2)P/T^2$	-	+	-	+	-	+	-	+
SM-4	$K_{m,m}T^3$	$K_n(K_{m,m}T^3)M_x/T^3$	\\\	\\\	\\\	\\\	-	-	+	+
SM-2	$K_{m,b}T^3$	$K_b(K_{m,b}T^3)M_x/T^3$	\\\	\\\	\\\	\\\	-	+	+	-
SM-4	$K_{m,m}T^3$	$K_n(K_{m,m}T^3)M_z/T^3$	-	-	+	+	\\\	\\\	\\\	\\\
SM-2	$K_{m,b}T^3$	$K_b(K_{m,b}T^3)M_z/T^3$	-	+	+	-	\\\	\\\	\\\	\\\
SV-4	$K_{m,m}T^2$	$K_n(K_{m,m}T^3)V_x/T^2$	-	-	+	+	\\\	\\\	\\\	\\\
SV-2	$K_{m,b}T^2$	$K_b(K_{m,b}T^3)V_x/T^2$	-	+	+	-	\\\	\\\	\\\	\\\
SV-4	$K_{m,m}T^2$	$K_n(K_{m,m}T^3)V_z/T^2$	\\\	\\\	\\\	\\\	-	-	+	+
SV-2	$K_{m,b}T^2$	$K_b(K_{m,b}T^3)V_z/T^2$	\\\	\\\	\\\	\\\	+	-	-	+
P		$pR_m/(2T)$								
Sum of meridional stresses										
ST–1	$K_{ts}T^2$	$(K_{ts}T^2)M_T/T^2$	+	+	+	+	+	+	+	+
SV–5	$K_{vs}T^2$	$(K_{vs}T^2)V_Z/T^2$	+	+	-	-	\\\	\\\	\\\	\\\
SV–5	$K_{vs}T^2$	$(K_{vs}T^2)V_X/T^2$	\\\	\\\	\\\	\\\	-	-	+	+
Sum of shear stresses										
Sigma1 (Max. principal stress) Sigma 2 (Min. principal stress) Sigma 3 (Internal pressure)			\\\		\\\		\\\		\\\	
Stress Intensity										
Maximum Stress intensity =										

Table I. Stress Computation Table for Sphere-Nozzle

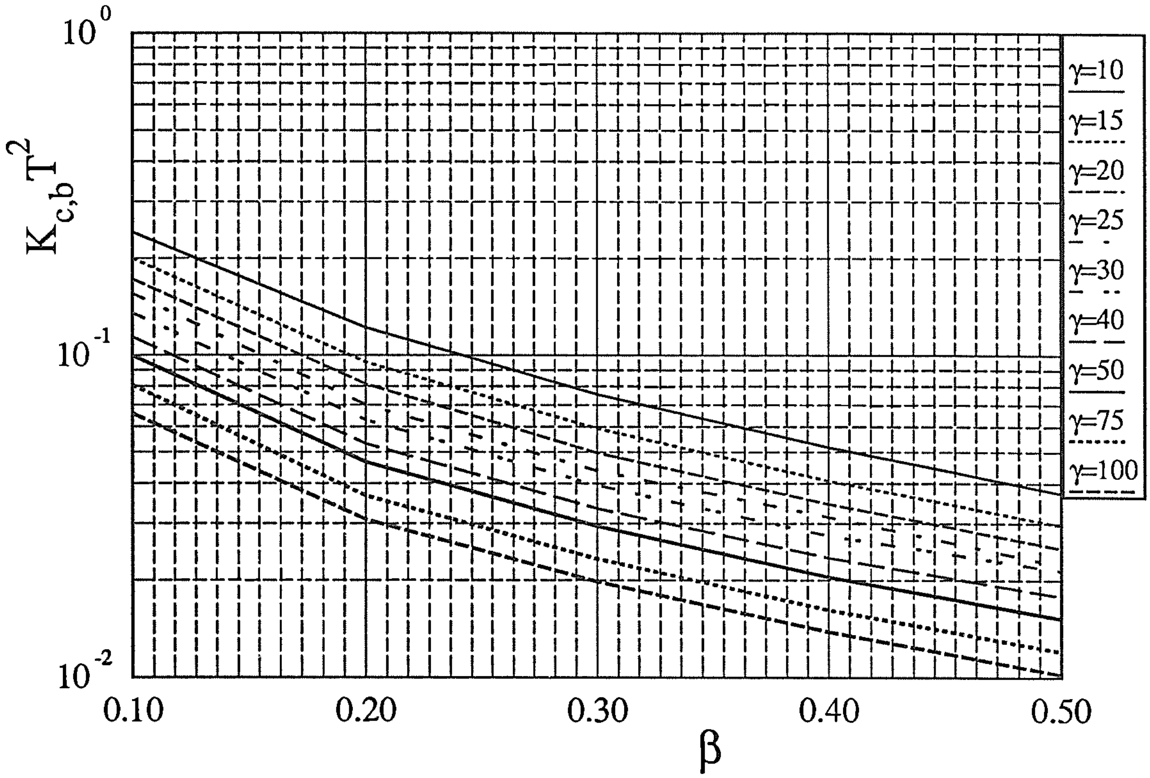

Figure SP-1 Circumferential Bending Stress Factor due to Radial Force

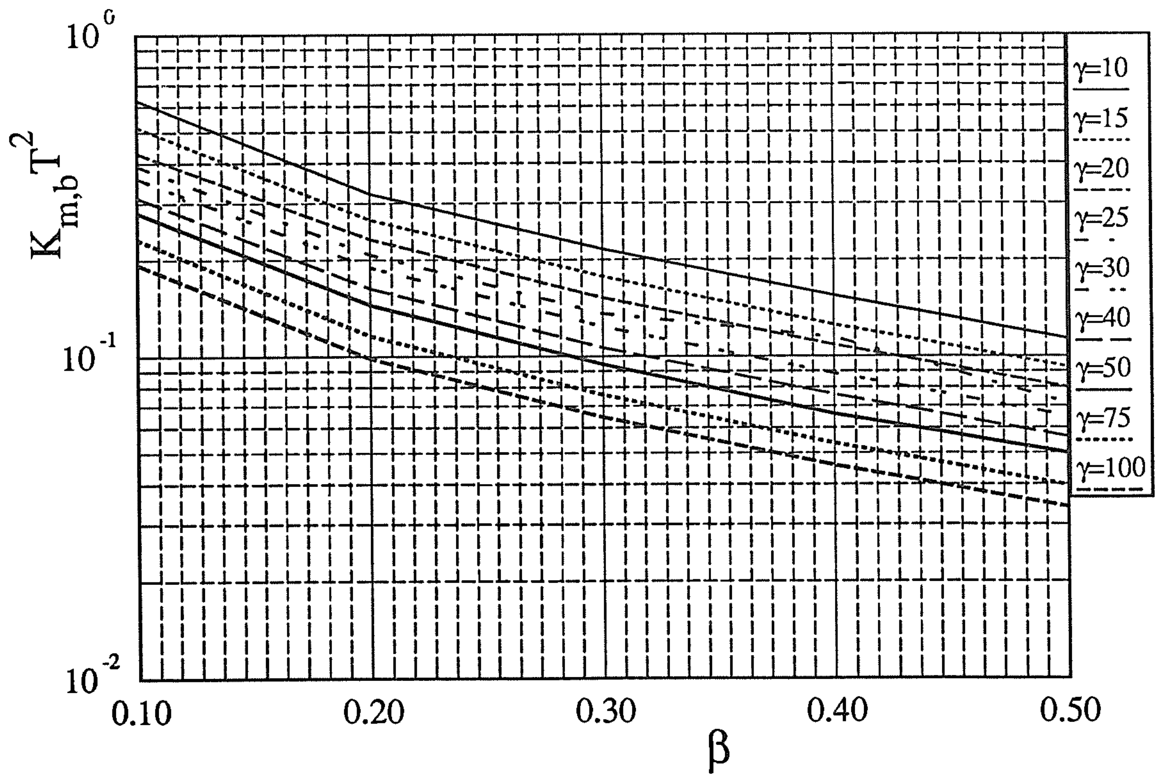

Figure SP-2 Meridional Bending Stress Factor due to Radial Force

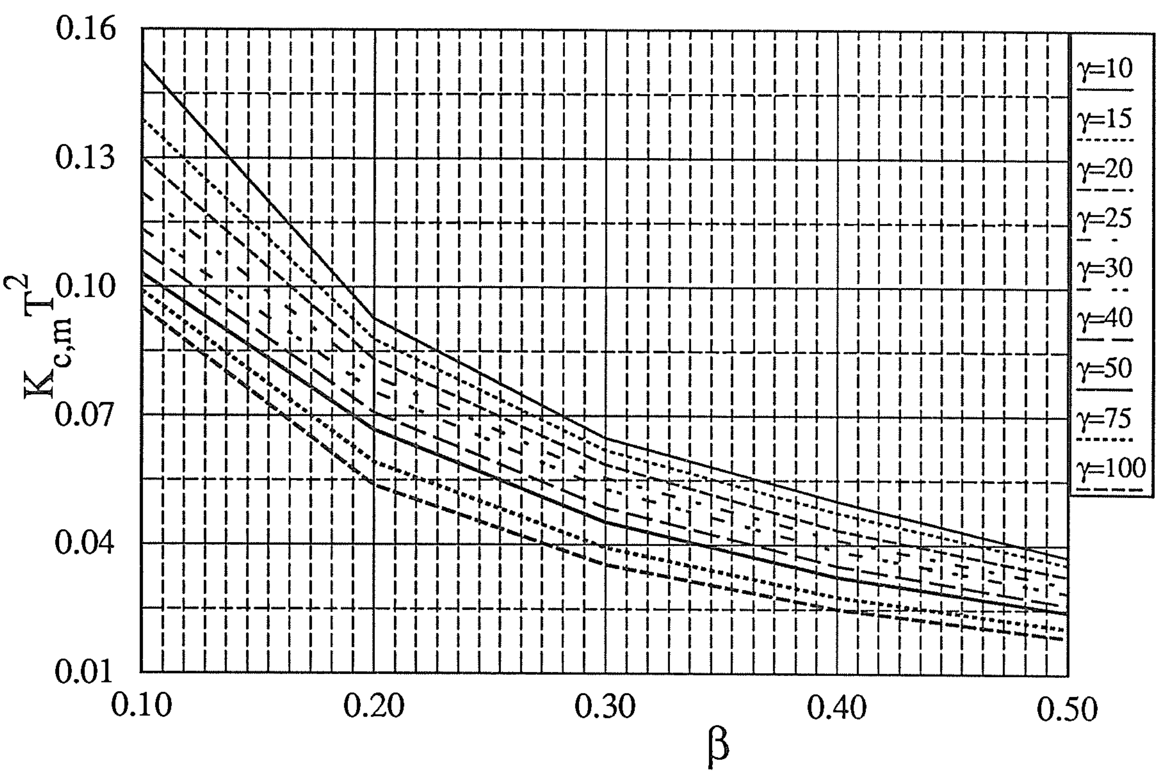

Figure SP-3 Circumferential Membrane Stress Factor due to Radial Force

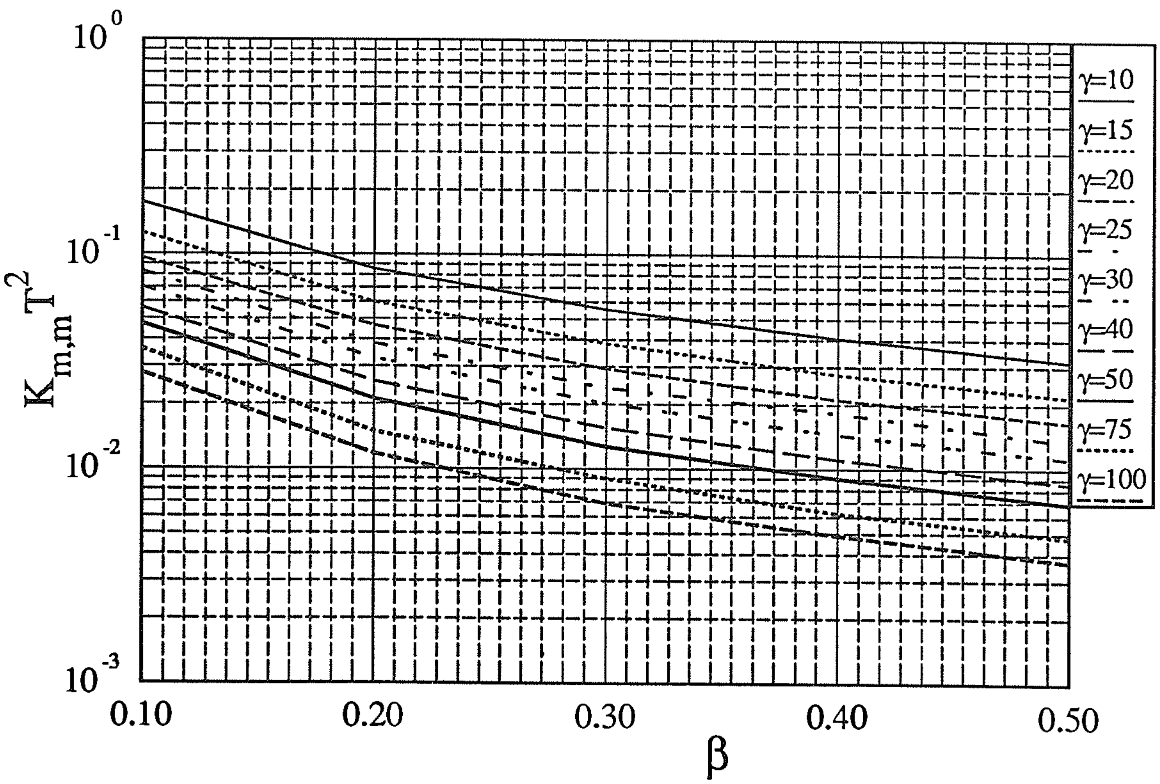

Figure SP-4 Meridional Membrane Stress Factor due to Radial Force

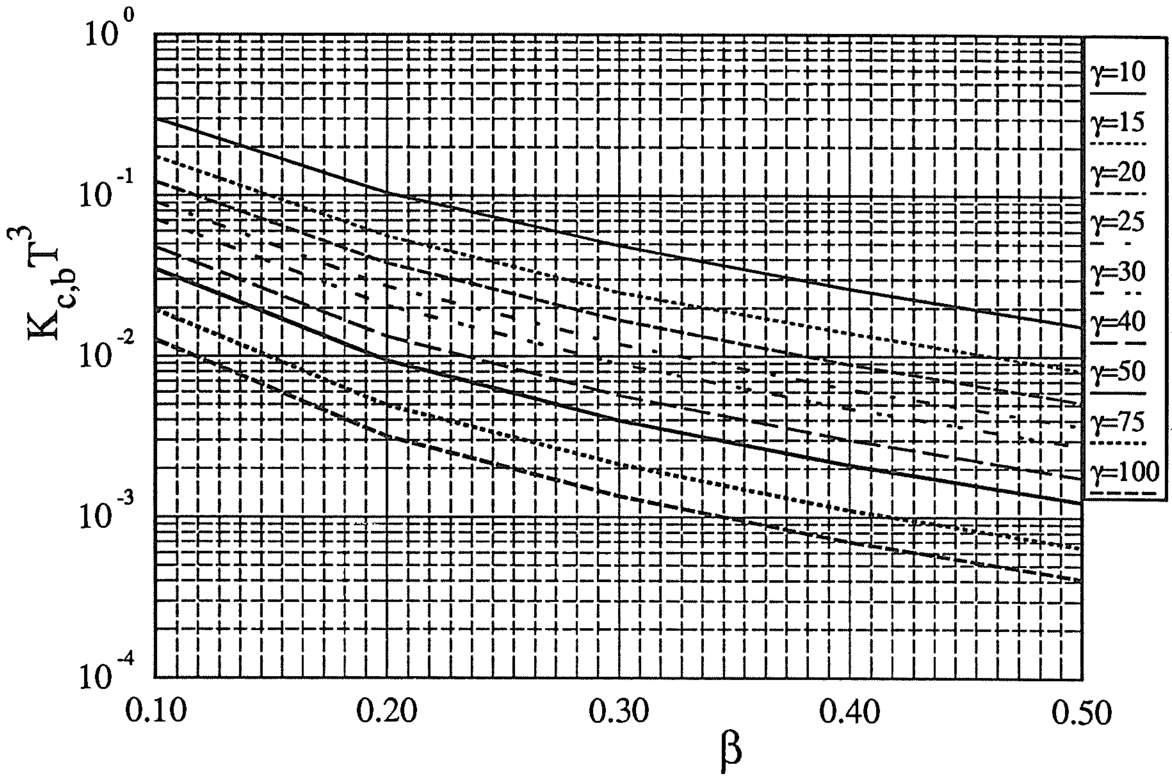

Figure SM-1 Circumferential Bending Stress Factor due to Overturning Moment

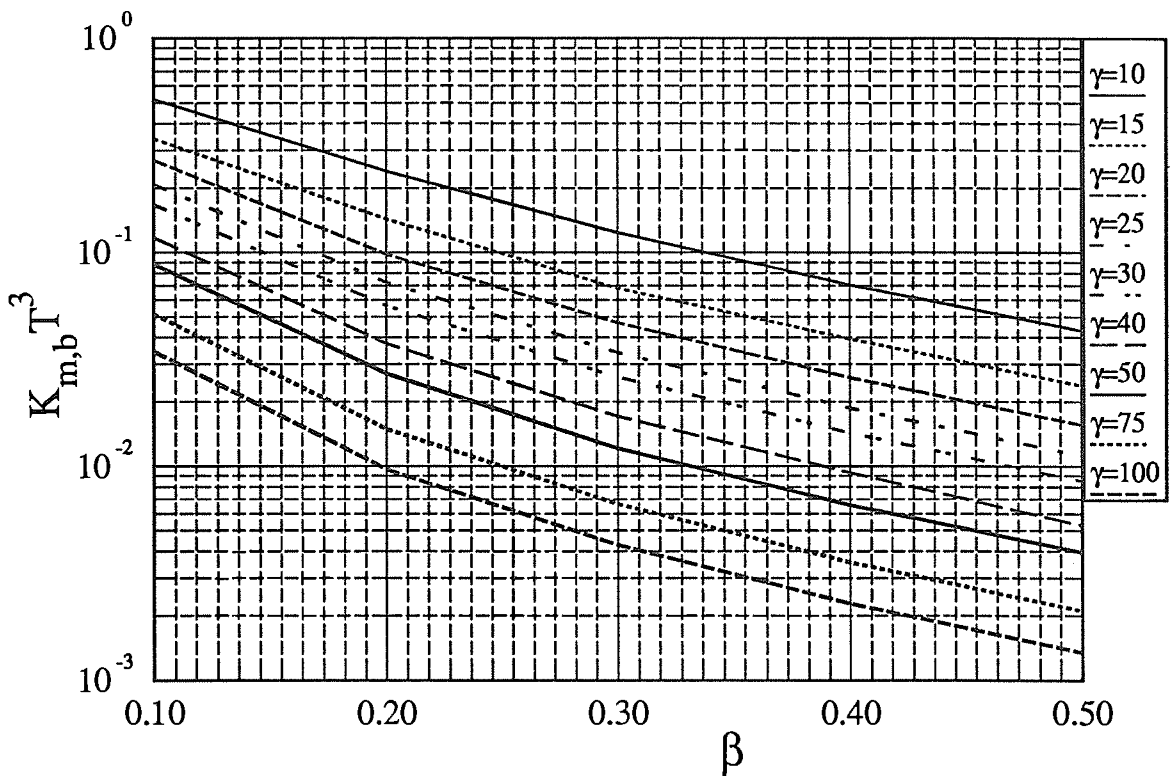

Figure SM-2 Meridional Bending Stress Factor due to Overturning Moment

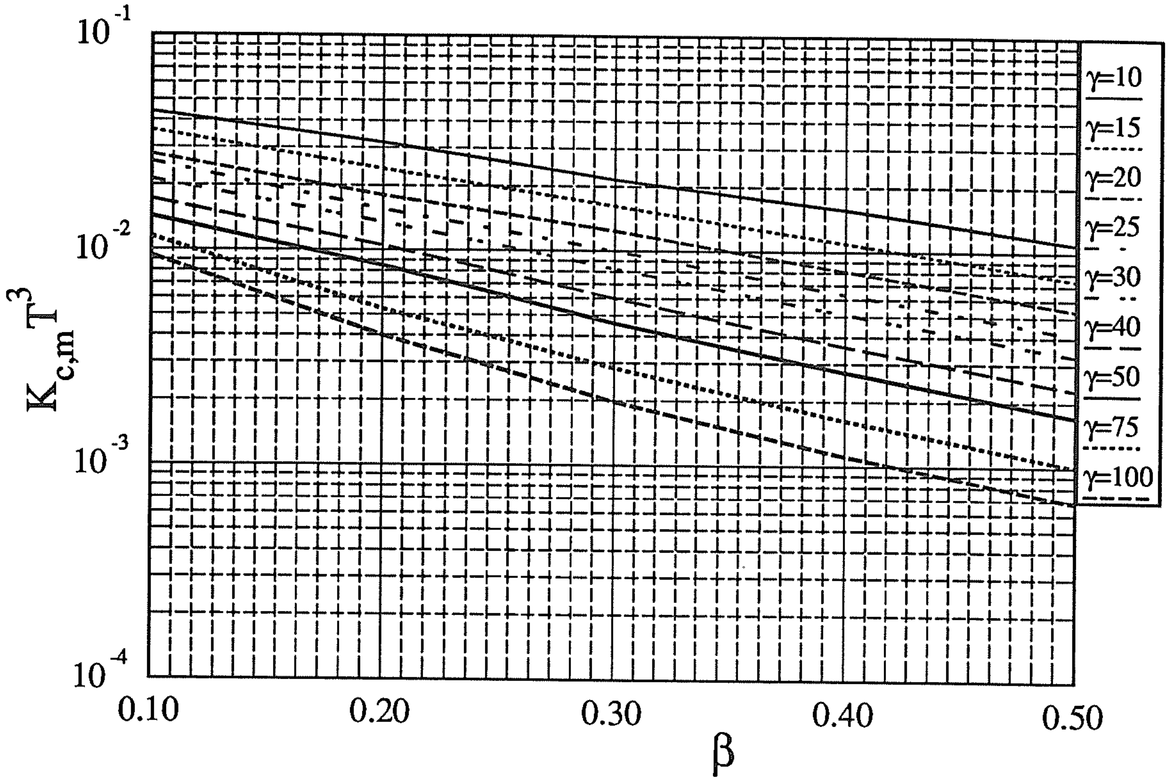

Figure SM-3 Circumferential Membrane Stress Factor due to Overturning Moment

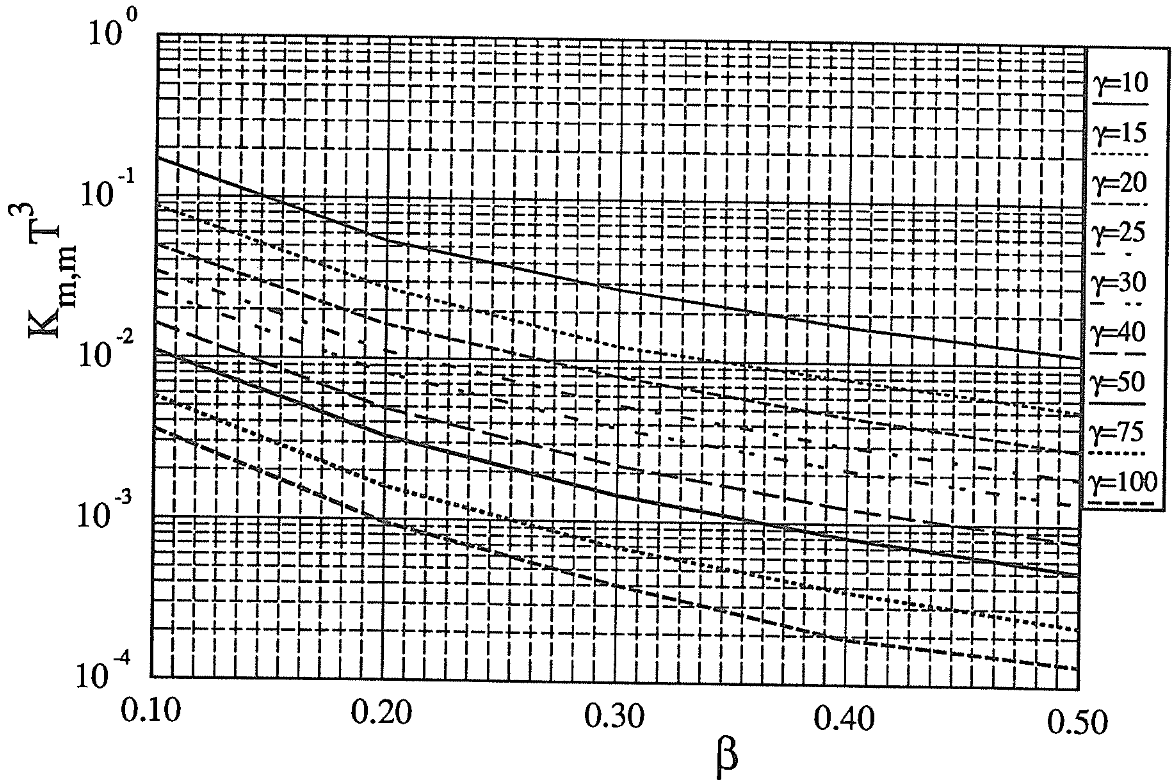

Figure SM-4 Meridional Membrane Stress Factor due to Overturning Moment

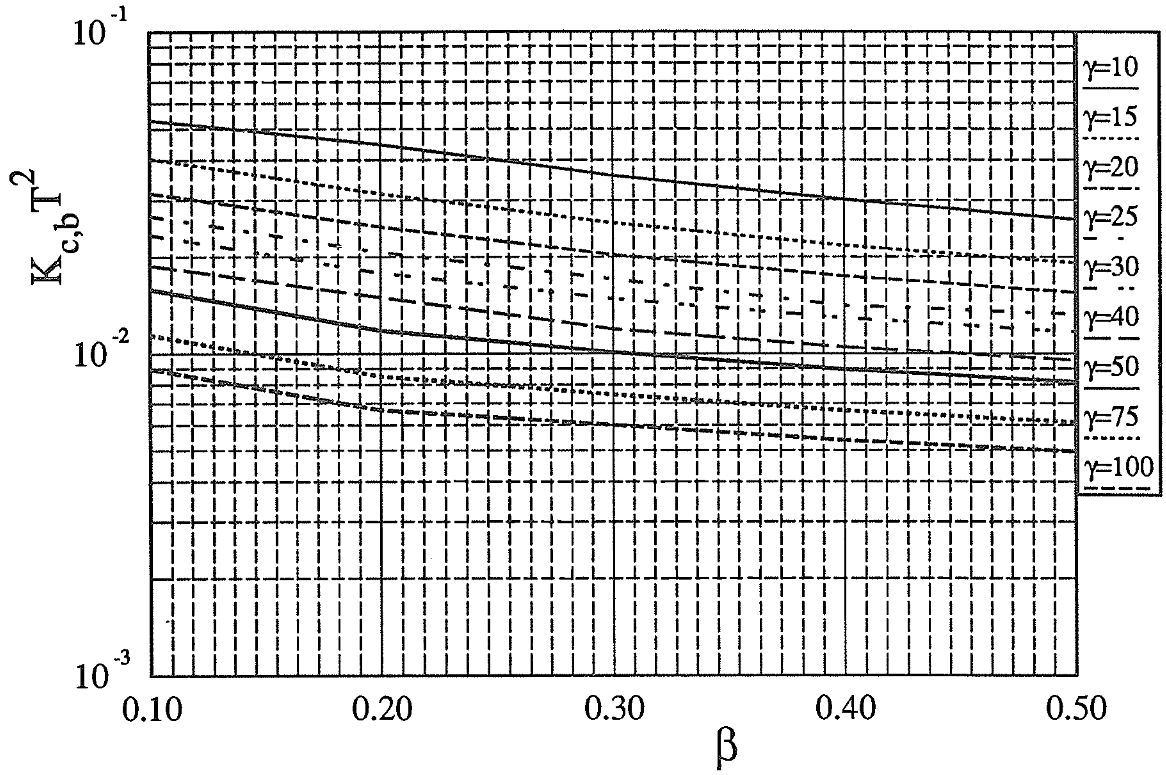

Figure SV-1 Circumferential Bending Stress Factor due to Horizontal Shear Force

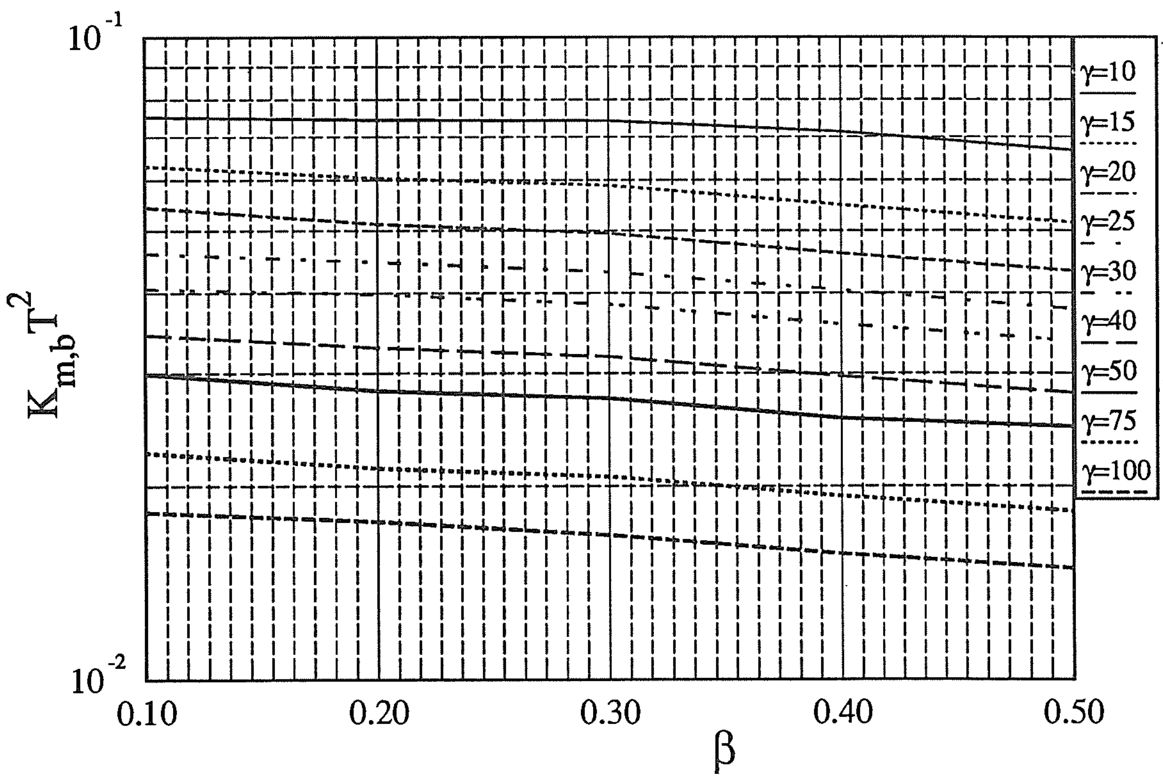

Figure SV-2 Meridional Bending Stress Factor due to Horizontal Shear Force

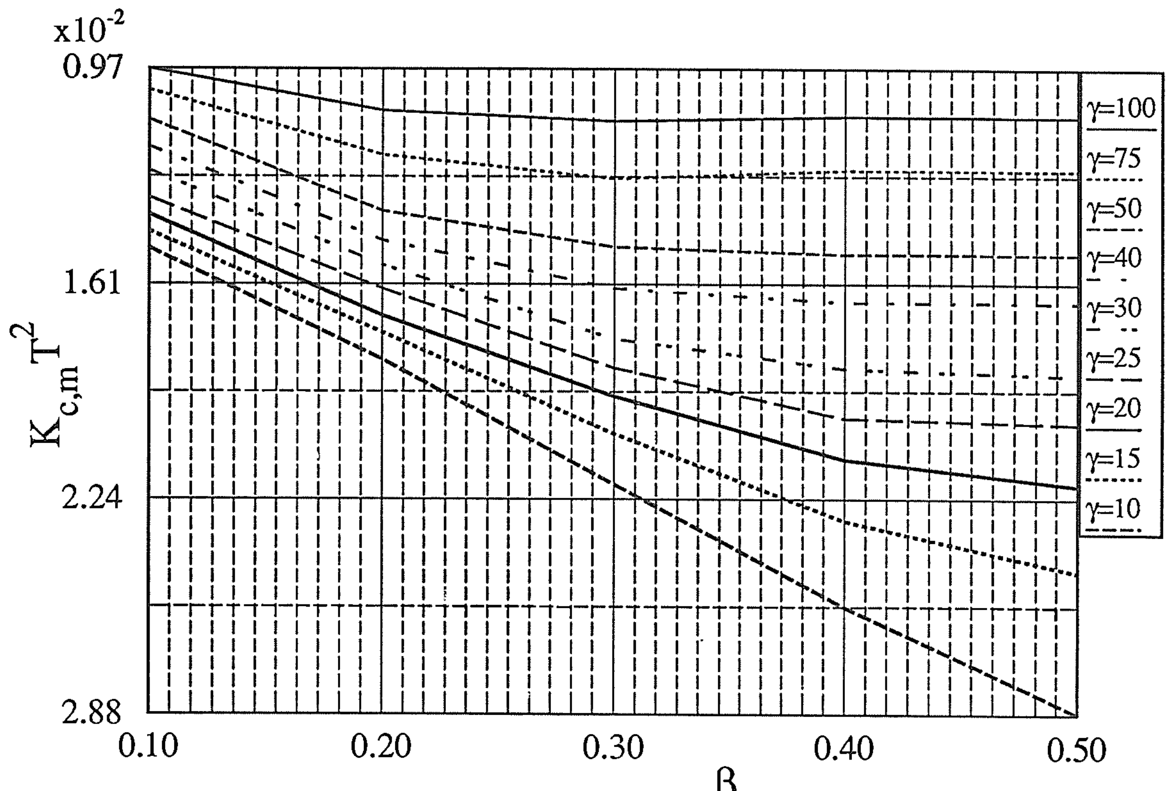

Figure SV-3 Circumferential Membrane Stress Factor due to Horizontal Shear Force

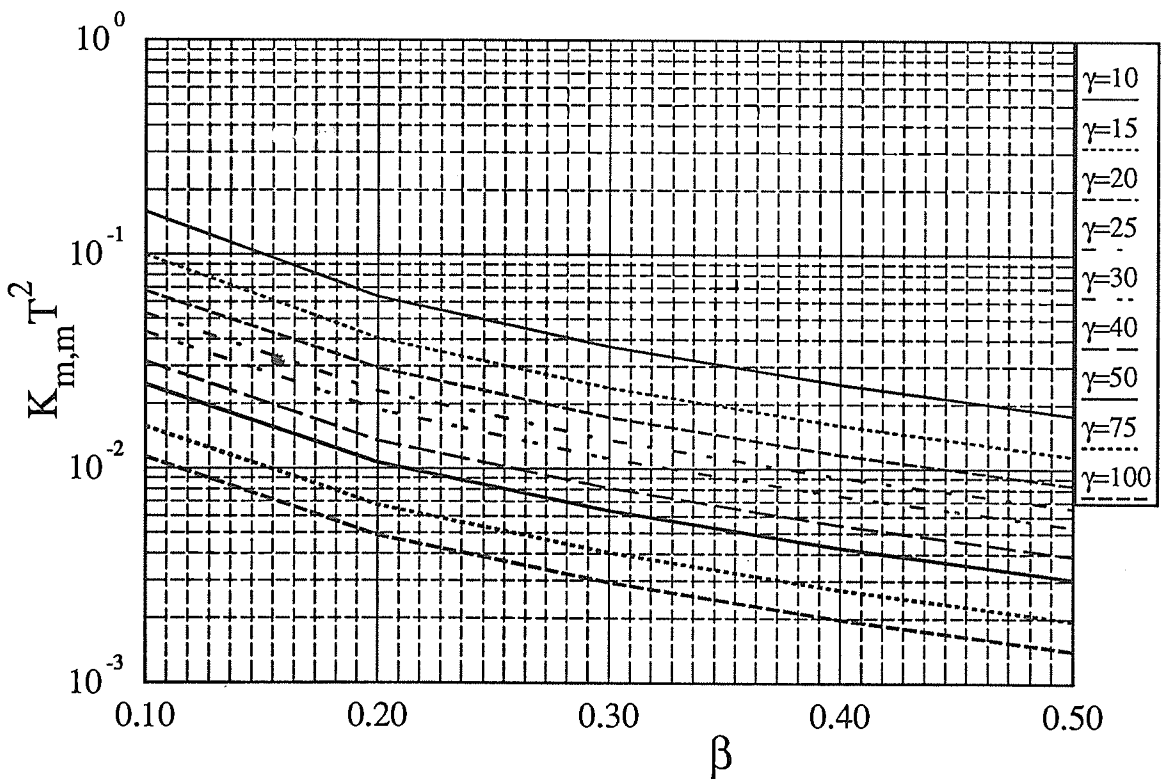

Figure SV-4 Meridional Membrane Stress Factor due to Horizontal Shear Force

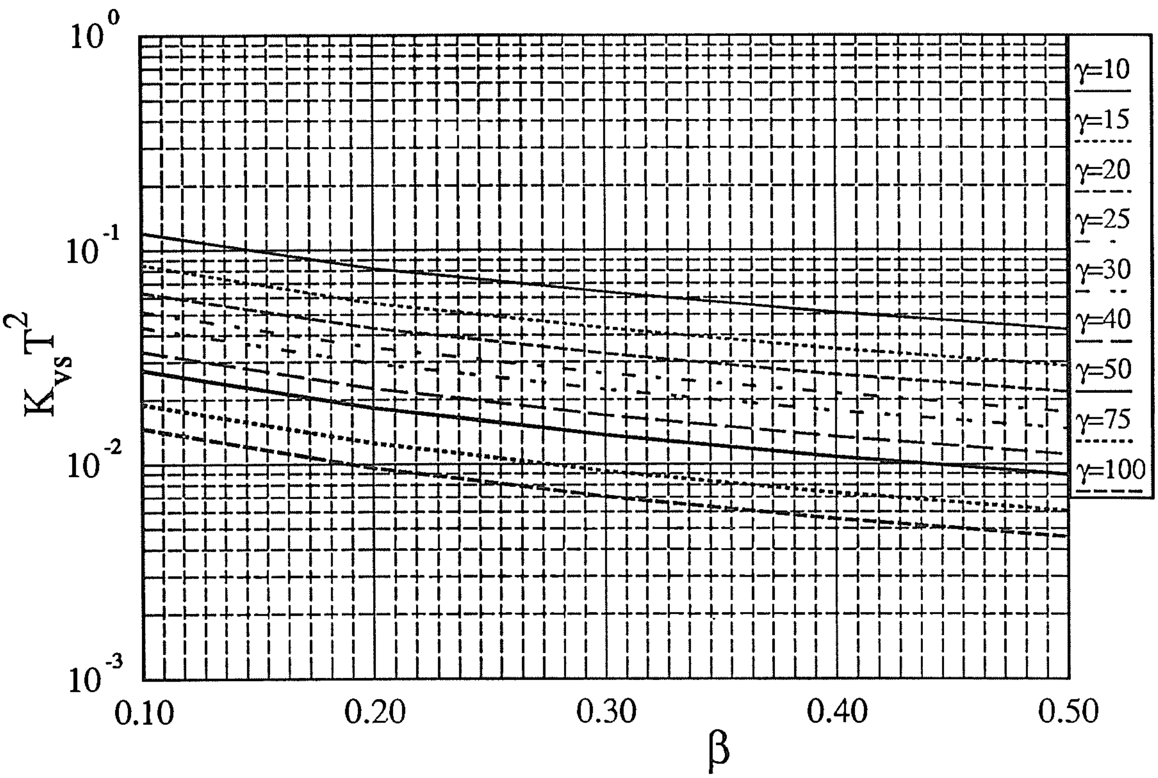

Figure SV-5 Shear Stress Factor due to Horizontal Shear Force

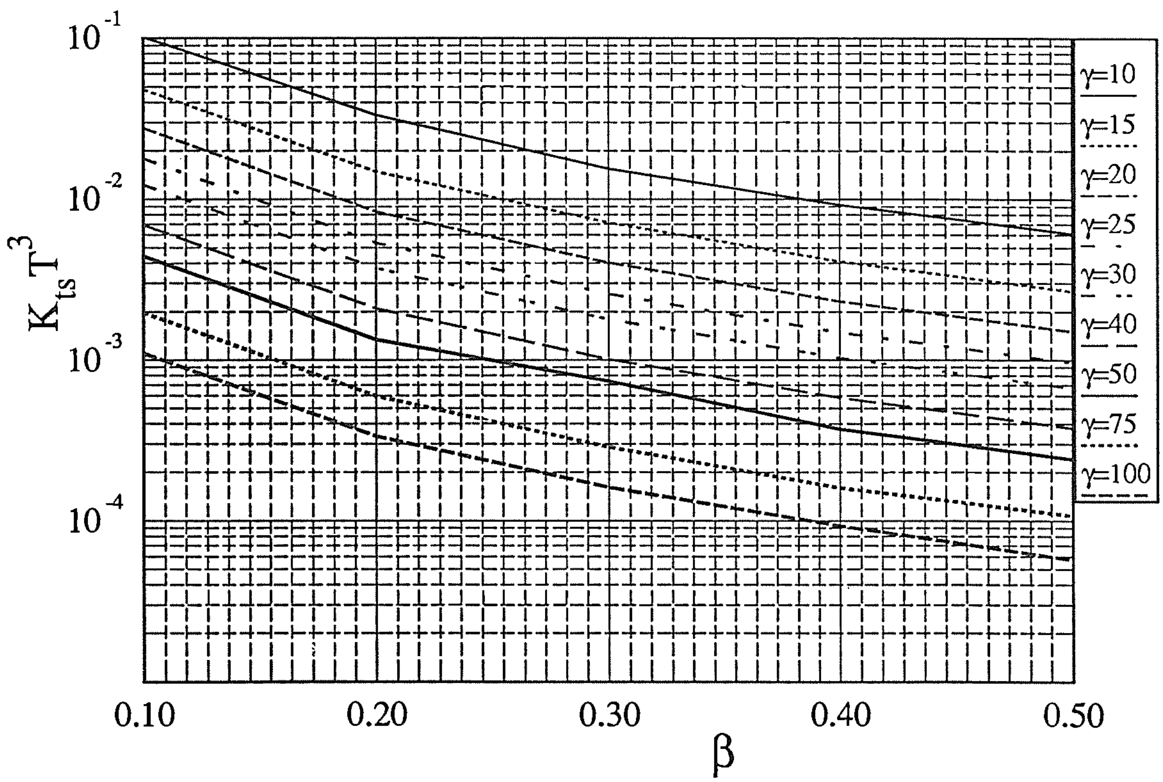

Figure ST-1 Shear Stress Factor due to Torsional Moment